CHALMERS
UNIVERSITY OF TECHNOLOGY

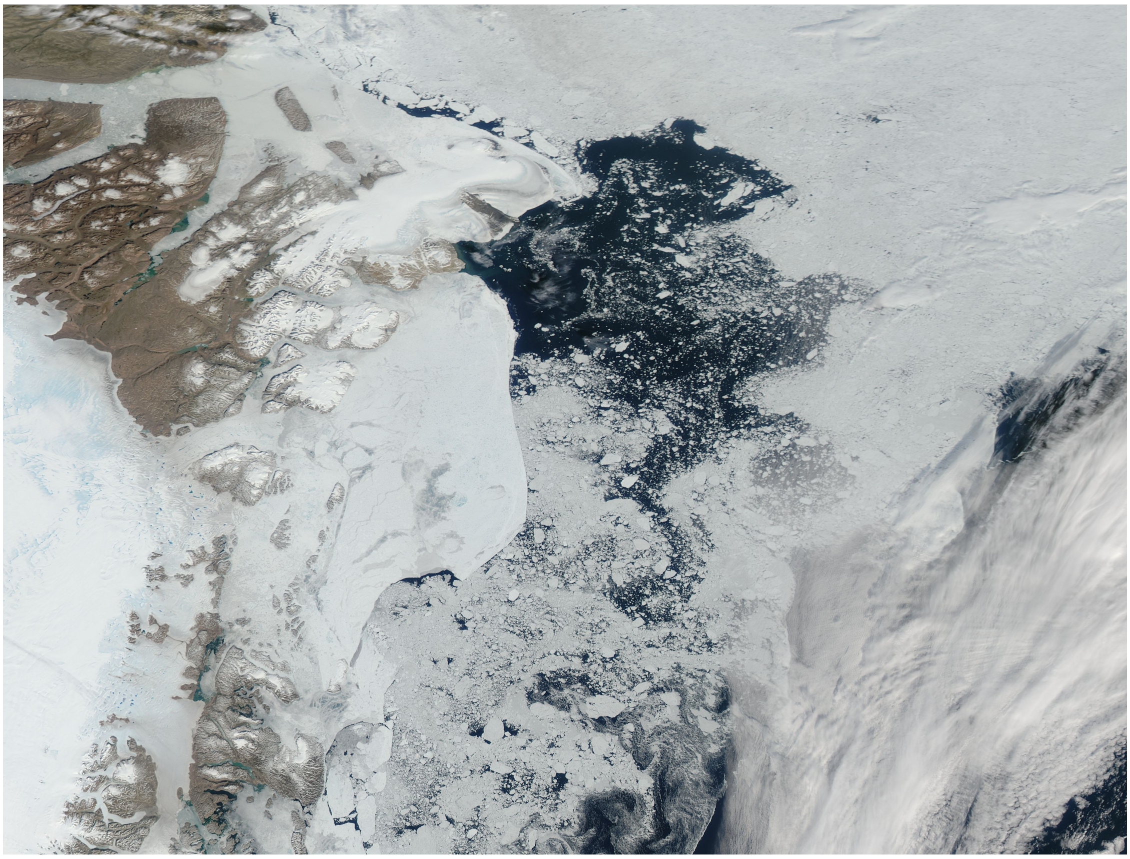

On the Relationship of Arctic Polynyas and Atmospheric Rivers

Analyzing Arctic polynya and atmospheric river activity during winter seasons between 1979 and 2019

Batchelor's thesis, Global Systems Engineering

Judit Engelsson, Martine Strandvik, Tyra Winnes

Chalmers University of Technology
Gothenburg, Sweden 2026

BACHELOR'S THESIS REPORT 2026

On the Relationship of Arctic Polynyas and Atmospheric Rivers

Analyzing Arctic polynya and atmospheric river activity during winter seasons between 1979 and 2019

Judit Engelsson, Martine Strandvik, Tyra Winnes

CHALMERS
UNIVERSITY OF TECHNOLOGY

Department of Space, Earth and Environment
CHALMERS UNIVERSITY OF TECHNOLOGY
Gothenburg, Sweden 2026

On the Relationship of Arctic Polynyas and Atmospheric Rivers
Analyzing Arctic polynya and atmospheric river activity during winter seasons between 1979 and 2019
Judit Engelsson, Martine Strandvik, Tyra Winnes

Supervisors: Erik Holmgren, Department of Space, Earth and Environment (Chalmers University of Technology), Carmen Hau Man Wong, Department of Earth Sciences (Univeristy of Gothenburg)
Examiner: Luisa Ickes, Department of Space, Earth and Environment (Chalmers University of Technology)

Bachelor's thesis report 2026
Department of Space, Earth and Environment
Chalmers University of Technology
SE-412 96 Gothenburg
Sweden
Telephone +46 31 772 1000

Cover: "Sea ice in the Greenland Sea" by NASA Goddard Photo and Video is licensed under CC BY 2.0. Cropped from original.
Typeset in LaTeX
Gothenburg, Sweden 2026

Abstract

Atmospheric rivers [ARs] are narrow and long regions characterized by unusually high moisture transport. ARs have over the last decades experienced a poleward shift and are because of this becoming more important to study in the higher latitudes. Arctic polynyas, openings in the sea ice cover, have simultaneously increased in frequency. However, the effect of ARs on arctic polynyas have not been sufficiently studied. In this study, we investigate the potential relationship between ARs and Arctic polynyas.

Using a public dataset based on satellite data and one AR-catalogue from the ARTMIP project, we retrieved polynya and AR activity for the winter seasons between 1979 and 2019. Initially, an Arctic-wide analysis was made. We analyzed the general characteristics of ARs and polynyas independent of their location. Then we examined the relationship between ARs and polynya opening events, here defined as the polynya variable changing from closed to open for any grid cell. Subsequently, we identified nine regions with high polynya activity and conducted a similar analysis for these individually.

Our results show a positive correlation ($r \approx 0.49$) between AR frequency and polynya opening events across the Arctic. Over a period of four days before the opening, ARs are present during approximately 36% of polynya opening events. This is a substantial increase compared to the baseline AR occurrence, which is almost 7%. The relationship between ARs and polynya openings is strongest one day prior to the opening event.

The regional analysis reveals high variability, with five out of nine regions showing positive correlations between AR frequency and polynya opening events, while the four remaining exhibit weak or negative correlations. The highest correlation is observed in Franz Josef Land, which has a high amount of both polynya openings and ARs. Furthermore, the regions Kara Sea, Svalbard and Chukchi Sea show a large increase in AR activity over polynya opening locations during the upcoming days of the opening event.

These findings suggest that ARs contribute to the triggering or enhancement of polynya openings. Further investigation is needed, as investigating ARs' effect on polynya openings as opposed to expansion of already existing polynyas, to better understand the dynamics of Arctic polynyas and AR activity.

Contents

1 Introduction

During the last 40 years, the mean temperature in the Arctic has increased four times faster compared to the rest of the globe and the consequences of this temperature rise is not limited to the Arctic (Rantanen et al., 2022). For example, the melting of permafrost, land ice and sea ice as a result of higher temperatures might lead to more greenhouse gases, higher sea levels as well as changes of the ocean currents (McGuire et al., 2009; Previdi et al., 2021; Schuur et al., 2008; Shepherd et al., 2012). Another effect of global warming is a decrease in albedo as the ice melts, leading to changes in the Earth's energy balance. Because changes in the Arctic have a broad impact on the rest of the planet it is crucial to understand the phenomena taking place there and their interactions. Two phenomena that have become more frequent in the Arctic region over the past years are polynyas and atmospheric rivers. The possible relationship between these has not yet been explored in the Arctic and is thus a motivation for this study.

2 Background

2.1 Polynyas

According to Armstrong (1972) polynyas are defined as "any non-linear opening enclosed in (sea) ice", meaning areas of open water or areas with very thin ice sheets surrounded by solid ice. They occur in regions where thicker ice would be expected due to cold temperatures (Tamura & Ohshima, 2011). Polynyas can vary in size, covering areas between 10 and $10^5 km^2$ (Smith et al., 1990). Over the last four decades, polynyas in the Arctic has increased. The study by Wong et al. (2026) suggests that for many regions in the Arctic the polynya opening frequency has increased 1-2 times per decade during the last forty years.

Polynyas can be divided into two categories, sensible heat and latent heat polynyas. Both of these are openings in the sea ice but the mechanisms keeping the polynya open are different. Sensible heat polynyas are driven by warmer water preventing new ice from being created and in some cases melting already existing ice (Morales Maqueda et al., 2004). Furthermore, sensible heat polynyas are created in areas where the vertical mixture of water is strong, often in bays or straits with tidal activities.

According to Morales Maqueda et al. (2004), latent heat polynyas on the other hand are driven by strong winds or currents transporting the sea ice to other regions, keeping an area ice free. Latent heat polynyas are places of high ice production. The open water forming the polynya is generally warmer than the air. This leads to heat being transferred from the water to the air, causing sea ice to form. It was before believed that the latent heat released when the water freezes is what keeps the polynya open, this has however been proven wrong and therefore latent heat polynyas is a somewhat misleading name. As previously stated, it is rather strong wind and currents transporting new ice away that keeps the polynya open. Latent heat polynyas are therefore said to be mechanically driven. The process of ice continuously being transported away leads to creation of even more new sea ice. Latent heat polynyas are often created along coasts with strong offshore winds. They are often generated along landfast ice or glaciers extending into the ocean.

The most common polynyas in the Arctic are the latent heat polynyas and these play a crucial role for the Arctic ocean circulation. When the water at the surface freezes the ocean surface salinity increases due to salt not binding when the water freezes. This results in the surface water increasing in density and sinking. In the Arctic, this dense water plays an important part in the creation of the cold halocline layer [CHL] (Winsor & Björk, 2000). CHL is an ocean layer acting as a barrier between the cold and fresh surface layer and the warmer and saline water deep water, coming from the Atlantic ocean (Morales Maqueda et al., 2004). This reduces convection between the cold surface water and warmer deep water, preventing ice in the Arctic to melt. However, the dense cold water from ice production in latent heat polynyas also enables ventilation between the deep water layers beneath the CHL (Schauer & Fahrbach, 1999).

Polynyas are not only important for the ocean circulation and stratification. They also play a crucial role for the heat flux between the air and the ocean (Morales Maqueda et al., 2004). Polynyas enable heat and moisture transport from the ocean to the atmosphere, leading to changes in the atmospheric motion. In the winter, polynyas stand for up to 50% of the heat exchange between the ocean and the atmosphere.

In the Arctic, the opening of latent heat polynyas appears to be, as mentioned earlier, partially driven by strong winds. In addition to wind, air temperature play an important part, both as a precondition for the opening event but also for the size of the polynya (Wong et al., 2026). Both of these mechanisms are closely associated with a larger atmospheric phenomenon known as atmospheric rivers [ARs]. However, the correlation between ARs and polynyas has not yet been sufficiently investigated in the Arctic.

2.2 Atmospheric rivers

ARs are defined as narrow and very long corridors of unusually high moisture, transported horizontally through the atmosphere. They account for up to 90% of the total moisture transport from the tropics to the higher latitudes and polar regions (Zhu & Newell, 1998). Around 80% of ARs (Z. Zhang et al., 2019) are a product of low level jet streams, ahead of the cold front of an extratropical cyclone (Francis et al., 2020), characterized by a low pressure. The other 20% occur without a nearby extratropical cyclone, but then usually close to another source of moisture and an anticyclone (Z. Zhang et al., 2019), characterized by a high pressure. ARs are a key factor contributing to the melting of sea ice in both the Arctic and Antarctic, primarily due to the significant amount of poleward transported moisture and heat (Francis et al., 2020).

Over the past decades, ARs have increased in both hemispheres while simultaneously decreased in the mid-latitudes, resulting in a poleward shift (Z. Li & Ding, 2024). P. Zhang et al. (2023) states that more frequent AR events in the Arctic region will lead to more precipitation along with an increase in downward longwave radiation. These factors are causing the sea ice to melt rapidly and at the same time slowing down the seasonal recovery of the Arctic sea ice (P. Zhang et al., 2023). The increased amount of precipitation will have a noticeable effect by melting the surface layer of the sea ice, due to energy transfer from liquid precipitation to the ice. This process transfers heat to the ice which induces the surface layer to melt. The high amount of moisture transported within ARs increases the absorption and re-emission of longwave radiaton in the atmosphere. This increase the downward longwave radiation reaching the ice surface, enhancing the greenhouse effect in the Arctic (Francis et al., 2020), one of Earth's primary places of albedo. Changes in the Earth's reflecting surfaces (albedo) could, as mentioned in Section 1, impact the overall energy balance and lead to drastic changes in the climate.

Although ARs are known to contribute to melting sea ice, their direct effects on polynyas have not yet been investigated explicitly in the Arctic. Understanding the relationship between ARs and polynyas is of great significance, especially in the context of global warming. An increase in ARs and polynyas could potentially lead to less ice coverage for both poles. This is because latent heat polynyas is a place for ice regrowth, while ARs could potentially hinder this process.

2.3 Regional characteristics in the Arctic

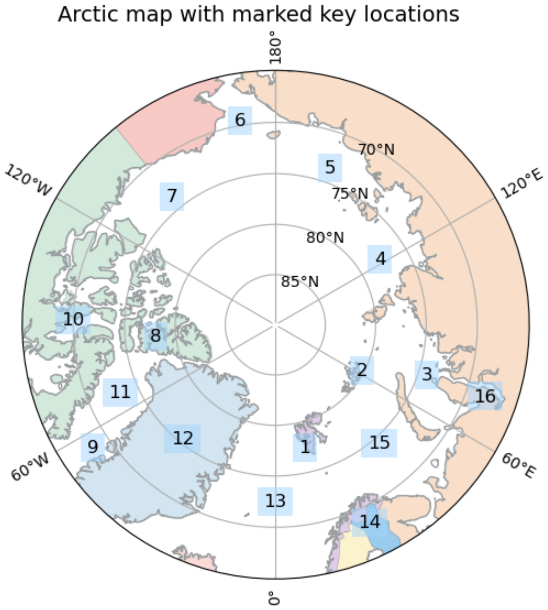

Number	Region
1	Svalbard
2	Franz Josef Land
3	Kara Sea
4	Laptev Sea
5	East Siberian Sea
6	Chukchi Sea
7	Beaufort Sea
8	North Open Water
9	Davis Strait
10	Canada
11	Baffin Bay
12	Greenland
13	Norwegian Sea
14	Scandinavia
15	Barents Sea
16	Russia

Figure 1: Map of the Arctic with key regions, with a table of mentioned regions names.

2.3.1 Forces driving polynyas in different regions

Polynya locations in the Arctic have various characteristics, where factors as wind, land ice, ocean currents and salinity affect the polynyas. The following section describes regional differences between polynya locations in the Arctic and how these are affected by different factors.

The Canadian coastline facing the Beaufort Sea (See Figure 1, (7)) experiences "outstanding high ice production", according to Winsor and Björk (2000). This is mainly due to frequent offshore winds, highlighting the importance of both wind and wind direction. Y. Zhang et al. (2021) states that the correlation between wind and the extent of polynyas were greater than the correlation with ocean heat transport in the East Siberian Sea 1, (5)). The same report also concluded that both wind speed and wind direction were important factors affecting the polynyas. In the East Siberian Sea (Figure 1, (5)), the dominant factor was wind direction, while the dominant factor in Chukchi Sea (Figure 1, (6)) was the wind speed. Wind appear to trigger polynya openings in some regions, but the speed and direction seems to be the key factors, varying between different regions.

According to Winsor and Björk (2000) polynyas might form off the Greenland coast and Canadian archipelago (Figure 1, (11)) along landfast ice. This implies that polynyas can form further away from the coast and not directly by the shoreline. High pressure and ice stress in glaciers, as those found on Greenland, can induce ice deep within the glacier to move in a flowing motion (Kump et al., 2014). On Greenland specifically, the land ice tends to flow into valley glaciers that end in the ocean, which can create large stresses in the sea ice (Kump et al., 2014; Winsor & Björk, 2000). They further emphasizes that elevated ice stress can inhibit the opening of polynyas. Such ice stress can be due to onshore or offshore ice drift driven by glacier flow, as well as strong winds or ocean currents. The region Davis Strait, south of North Open Water (Figure 1, (8),(9)), could inhabit polynyas along the Arctic ice edge (Wong et al., 2026) misinterpreted as real polynyas. Polynya regions close to the seasonal ice edge, like Davis Strait (Figure 1, (9)), can therefore yield an overestimated polynya frequency.

Apart from glacier impacts, Baffin Bay (Figure 1, (11)) experiences cold currents entering from the Labrador Sea, the Labrador Current (Kump et al., 2014). The regions Svalbard, Kara Sea and Franz Josef Land (Figure 1, (1),(2),(3)) on the other hand, all experience a warm current, the North Atlantic drift moving in from the North Atlantic through the Norwegian Sea (Figure 1, (13)). There is also a large gyre in the Beaufort Sea (Figure 1, (7)), called the Beaufort Gyre, which affects the drifting sea ice in the region, possibly circulating for long periods of time (Kump et al., 2014).

A common factor revealing if a region has active polynyas or not, is the salinity levels, since high increases in salinity throughout the season is directly related to ice production (Winsor & Björk, 2000). According to Winsor and Björk (2000) regions with the lowest increase in salinity are located along the Canadian archipelago and the Greenland coast (Figure 1, (11)), partially in North Open Water (Figure 1, (8)), suggesting less polynya activity there. Previously known polynya locations, Kara Sea, Svalbard and Franz Josef Land (Figure 1, (1),(2),(3)), all in the vicinity of Barents Sea (Figure 1, (15)) have the highest initial salinity. Even a modest increase results in a high final salinity. Regions with the lowest initial salinity are Laptev Sea and the East Siberian Sea (Figure 1, (4),(5)), whereas the salinity increase in Laptev Sea suggests an active polynya region.

The polynya regions in the Arctic also differ in seasonal behavior, some regions have polynyas opening up early and others late in the winter season. Winsor and Björk (2000) brings up the regions Kara Sea, Franz Josef Land and Svalbard (Figure 1, (1),(2),(3)) as being ice free further into the winter season than other regions. This is in line with the results by Wong et al. (2026), showing slightly more polynya openings in February and March, when the Arctic seasonal ice cover has formed there. The report also show that polynyas in the East Siberian Sea and Chukchi Sea (Figure 1, (5),(6)) opens early in the season, primarily in December (Wong et al., 2026).

2.3.2 Impact of ARs in the Arctic

Previous studies have shown that the moisture ARs transport to the Arctic have a large impact on the sea ice variations in the region (L. Li et al., 2024). The energy budget is, as stated before, affected due to the increased water vapor blocking and re-emitting longwave radiation back to the surface. In the Arctic, this effect is greater in the winter compared to the summer. This means that, even though the AR activity is lower in winter, they have a greater effect on the ice variations during the winter.

One example showing the effect ARs have on the Arctic ice cover is the melting of land ice in the region. A study by Mattingly et al. (2018) shows that ARs increase the melting of the Greenland ice sheet. Strong individual ARs seemed to have a direct effect of the melting of the ice sheet. Furthermore, the case study by Haacker et al. (2024) exploring ARs impact on glaciers in Novaya Zemlya (an archipelago in the Kara Sea, northern Russia) shows that 71% ś 3% of the melting of ice was driven by ARs. The correlation between the yearly melt of glaciers and the moisture transport in the region increased from $r = 0.07$ in the years 1981-2010 to $r = 0.63$ in 2011-2022, indicating that moisture transport is becoming a more important factor in glacier melt. Even though these examples investigates land ice and not sea ice, they still show the effects that ARs have on the ice sheet in the Arctic.

It has also been shown that ARs are linked to extreme warming events in the Arctic. Ma et al. (2024) defines an extreme warming event in the Arctic as the temperature 2 meters above ground being over 0 řC. These events are mainly present in the Norwegian Sea, Barents Sea and Kara Sea. However, the study shows that for many regions in the Arctic, all of the extreme warming events detected in the time period 1980-2020 coincided with AR activity.

2.4 AR detection algorithms and reanalysis products

Over the years, scientists have used different methods and algorithms to detect ARs. Today the Atmospheric River Tracking Method Intercomparison Project (ARTMIP; Shields et al. (2018)) is trying to create a framework that let users compare different AR identification methods, understand the uncertainties of these methods and provide the best detection-methods for various fields. The project includes comparison of 34 AR detection algorithms and consists of two steps, Tier 1 and Tier 2. In Tier 1, all algorithms are run on the same dataset, MERRA v2 Reanalysis. In Tier 2, the participants may run their algorithms on various reanalysis products to investigate how sensitive the results are for the choice of dataset and to study how ARs are affected by climate change.

Reanalysis products are created using data assimilation, which combine observed data with weather models to create a complete picture of the weather over time. The weather model produces a forecast for a specific time step and then the initial conditions of the model are adjusted to fit actual observations. The adjusted model is then used to produce a forecast of the next time step, making the process iterative (European Centre for Medium-Range Weather Forecasts, 2025). The complete view of the weather over time is the reanalysis product. It includes parameters that describe the ocean, the atmosphere and the Earth's surface (Copernicus Climate change service, n.d.). One of the most commonly used climate reanalysis datasets is ERA5 (Service, 2023) which is produced by the European Centre for Medium-Range Weather Forecasts [ECMWF]. The ERA5 dataset comprise hourly data from 1940 onwards, with a spatial resolution of 31 km (Hersbach et al., 2020). AR detection algorithms are commonly run on reanalysis products such as ERA5 to generate so called AR catalogues. AR catalogues contain the detected ARs in each timestep for every included grid cell.

3 Aim

Both Arctic polynyas and ARs are influenced by numerous atmospheric and oceanic processes. Previous sections have outlined the individual characteristics of these phenomena, but their potential interdependence is insufficiently researched. With this reasoning, the aim of this study is to identify and investigate a possible relationship between polynyas and ARs in the Arctic.

In order to fulfill the purpose of this study, it is necessary to examine whether a statistical relationship between Arctic polynyas and ARs can be identified. Furthermore, the possible relationship will be investigated by analyzing both phenomena's seasonal frequencies as well as ARs close in time to locations where polynyas occur.

Consequently, the overall problem is broken down into a set of more specific research questions addressing the nature and definition of the potential relationship between Arctic polynyas and ARs.

1. How are ARs and polynyas spatially distributed in the Arctic?
2. How has ARs and polynya activity varied in the Arctic over the last 40 years?
3. How is polynya activity affected by ARs;
   (a) Independent of the location of both phenomena?
   (b) Passing directly over the polynya?

4 Data and methodology

4.1 Polynya and AR datasets

In this study we used two datasets, one with polynya data and one with AR data. The datasets contain a binary mask of polynya/AR activity. For every data point, the value is set to one if a polynya/AR is present and zero if not. The following section explains how these datasets are produced.

4.1.1 Polynya dataset

The polynya dataset is retrieved from satellite data of sea ice concentrations from Nimbus-7 SMMR and DMSP SSM/I-SSMIS Passive Microwave Data, (Wong & Heuzé, 2025). It consists of three dimensions; latitude, longitude and time. The parameter used to detect polynyas is sea ice concentration (SIC), with a threshold value of 20%. This means that if the SIC-value is below 20%, the polynya dataset change from closed (0) to open (1) for that grid cell and timestamp. The temporal resolution is daily, with an exception for the first eight years where there are missing values every other day. It includes data for the winter seasons (December, January, February and March), between 1978 and 2024.

This report discusses the polynyas located in the Arctic and therefore it is of relevance to define what is geographically included in the Arctic region. The most common definition is that the Arctic is the area within the Arctic circle, situated at latitude 66.3°. Hence, the northern parts of Scandinavia, Russia, Canada, Alaska and Greenland are included in the Arctic. The polynya dataset cover an area from latitude 65° to 90°, and therefore the entire dataset was used in this study.

4.1.2 AR dataset

We have used an AR catalogue published by the ARTMIP Tier 2 project (Shields et al., 2022) based on ERA5 reanalysis data (Hersbach et al., 2020) and the GuanWaliser v2 algorithm used for detection and tracking of ARs (Guan & Waliser, 2015, 2019). This algorithm uses threshold values for the integrated water vapor transport (IVT), which varies between regions and seasons. An AR is detected when the value of IVT is above the 85th percentile, for each grid cell (Guan & Waliser, 2015, 2019). However, this threshold value can not be below $100\,\mathrm{kg\,m^{-1}\,s^{-1}}$. There are also requirements on the geometry, where the length of the AR must be $> 2000\,\mathrm{km}$ and the length to width ratio > 2. Furthermore there is a threshold value for the direction of the AR, the mean direction have to be $> 50\,\mathrm{kg\,m^{-1}\,s^{-1}}$ poleward. The AR dataset contains hourly data for the entire planet with a grid size of 25x25 km. The period covered is from January 1979 through December 2019.

4.2 Rearranging the data

As stated in the previous section, the AR and polynya data does not cover the exact same time period. To be able to analyze and compare the phenomena, we chose a time period that is covered by both datasets. The period studied was the winter seasons (December, January, February and March) starting December 1st 1979 and ending March 31st 2019. This time period will further be referred to as our "time period of study".

The polynya file required further processing, as every other date was labeled as 'NaT' between 1979 and 1987. These were replaced with their corresponding days and their corresponding binary value was then set to 'nan' to not affect the results. The AR dataset had to be downsampled from hourly to daily, in order to align with the polynya dataset. Since ARs are a slow evolving phenomena, daily data is still meaningful for this analysis. Changing from hourly to daily data was done by assigning a value of 1 to every day that contained at least one hour with an AR present.

To be able to combine the datasets spatially, the polynya dataset was regridded to match the spatial resolution of the AR dataset. We did the regridding using the nearest neighbor method, source to destination (s2d) which assigns every new grid cell the value of the nearest grid cell in the old grid. Then, AR data from latitude 65° to 90° was extracted to match the polynya dataset.

4.3 Initial analysis of general AR and polynya characteristics

Once the datasets were resampled, an initial analysis was conducted. This involved computing the frequency over the whole time period of ARs and polynyas over the Arctic to see were these occur. This frequency can be understood as "The percentage of time (over the whole time period) that a grid cell has experienced a polynya/AR, for every grid cell".

The spatial average of polynya and AR activity in the Arctic were also calculated over time. When doing this, instead of calculating every data point, we created monthly means since this allowed easier visualization. This can be understood as "The percentage of the Arctic region covered by polynyas/ARs each month".

4.4 Defining and detecting polynya opening events

After the initial analysis, we increased the level of detail by studying the opening event of a polynya grid cell. In this report, we define the opening event as the polynya variable changing from 0 to 1 for a grid cell, regardless of the values in neighboring grid cells. This means that the opening events include both initial openings of polynyas and expansion of already existing polynyas. When finding the polynya openings, a new dataset was created. In this dataset, the value for the polynya variable was set to one if a polynya opening was detected and zero otherwise.

4.5 Correlation analysis

To investigate trends between AR activity and polynya openings, using the AR and polynya opening datasets, we summarized their activity for each season (December, January, February, March) over the Arctic. From this we calculated the seasonal frequency of both phenomena, represented by seasonal means. A linear regression between the seasonal frequencies, as well as the Pearson correlation coefficient and *p*-value, was calculated to facilitate the results. Section 4.5.1 explains how the Pearson correlation coefficient is calculated and how it can be interpreted. Section 4.5.2 explains how statistical significance is determined based on the *p*-value.

4.5.1 Pearson's correlation coefficient

Correlation calculations are used to establish statistical relationships (Temizel et al., 2011). The Pearson correlation coefficient, r, measures linear correlation between two data sets by applying the ratio between their covariances as well as the product of their standard deviations.

The calculation generates a value between -1 and 1 (Berman, 2016). A negative correlation close to -1 indicates that the data sets correlate inversely, while a positive correlation near 1 denotes a positive linear relationship. An r value around zero would imply that the data sets are uncorrelated.

The method assumes that the datasets both have a normal distribution, are independent from each other and have a linear relationship (Faizi & Alvi, 2023). Previous research has also shown that the correlation value is sensitive to outliers (Kim et al., 2015).

The formula for Pearson's correlation coefficient:

$$r = \frac{n(\sum xy) - (\sum x)(\sum y)}{\sqrt{[n(\sum x^2) - (\sum x)^2] - [n(\sum y^2) - (\sum y)^2]}} \tag{1}$$

4.5.2 Statistical significance

Calculating statistical significance is a method used to determine whether measured results are likely to be observed by some sort of chance (Priest, 2005). The method uses a null hypothesis, the chosen test statistic and the distribution of the test statistic under the null hypothesis to find a *p*-value (Reid, 2001). The null hypothesis assumes that no relationship exists between the two datasets. The findings can be described as follows:

> "The result of the test is to indicate whether the data are consistent with the null hypothesis: if they are not, then either we have observed an event of low probability, or the null hypothesis is not correct" (Reid, 2001).

It is important to note that a statistically significant result is not necessarily practically significant in a given analysis, for example because datasets with few data points often result in high *p*-values. However, a common consensus is to regard $p < 0{,}05$ as statistically significant.

4.6 Analysis with respect to location and time

The correlation analysis described in Section 4.5 did not consider the locations of ARs or polynya openings. The only time constraint in the analysis was that we only looked at occurrence during the same season. To narrow the analysis even further, we looked at ARs passing directly over polynya opening locations the days leading up to the opening event and on the day of the opening.

This was done by assessing the presence of ARs at the polynya opening locations. The analysis considered whether ARs were present in the days leading up to an opening event, as well as on the day of occurrence, in order to investigate a potential delayed relationship between ARs and polynya openings. A delay of this kind will throughout the report be referred to as time lag.

First, a collective analysis of all time lags were performed to estimate the general probability of AR presence prior to and on the day of polynya openings. For each opening event, it was determined whether an AR was present in the same grid cell any of the four days leading up to, or on the actual day, of the opening. If an AR was detected on any of these days, the event was counted once, without considering additional time lags for that same opening. This provided a measure of how frequently ARs occur close in time to polynya openings.

This measure was then compared to the general prevalence of ARs at these locations over the entire 40-year period. This was done by calculating how often ARs were present, for all polynya opening locations, regardless of when an opening event occurred. This percentage can be understood as a baseline of AR occurrence on polynya opening locations.

Second, the time lags were analyzed individually. By iterating over all opening events, the percentage of polynya openings coinciding with AR presence was calculated for each time lag separately. This provided a measure of how many days prior to the opening ARs were most common for each region.

4.7 Regional analysis

An analysis on a regional level made the spatial conditions narrower, allowing more specific conclusions to be made. Nine regions were identified through literature together with our results of polynya frequency over the Arctic. These regions are shown in Figure 2.

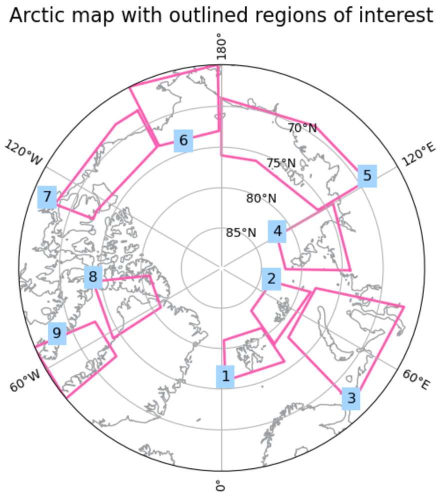

Number	Region	Longitid & latitud
1	Svalbard	2ř-34řE, 76ř-81řN
2	Franz Josef Land [FJL]	35ř-75řE, 78.5ř-83.5řN
3	Kara Sea	44ř-78řE, 67ř-78řN
4	Laptev Sea	89ř-120řE, 74ř-82řN
5	East Siberian Sea [ESS]	121ř-180řE, 69ř-76řN
6	Chukchi Sea	153ř-179řW, 65ř-73řN
7	Beaufort Sea	111ř-152řW, 68ř-73řN
8	North Open Water [NOW]	57ř-84řW, 74ř-81řN
9	Davis Strait	50ř-67řW, 65ř-73řN

Figure 2: Map of the nine regions used in the regional analysis of polynya and AR activity. Followed by a table with region names and coordinates for each region.

The correlation analysis explained in Section 4.5 and the narrower analysis of ARs passing directly over polynyas close in time of the opening event, explained in Section 4.6, were conduced for each of the nine regions.

5 Results and analysis

5.1 General AR and polynya characteristics

The following chapter shows how polynya and AR activity has been distributed over the Arctic region as well as how the frequency of these phenomena has changed over time.

5.1.1 Polynya and AR frequency

During the 40-year period, ARs reach the entire Arctic region (see Figure 3). Over the same period, polynyas have mainly been present along coastal regions with some minor indicators of polynyas at the center of the Arctic. The spatial patterns observed align with identified patterns in previous research. We see that both AR and polynya frequencies are higher in the same regions. ARs are more common in two regions, one being over the Chukchi Sea and the other over the Norwegian Sea stretching over northern Scandinavia and Russia. For the regions with the lowest frequencies, polynyas have only been present around 10 to 40 days throughout the entire period. Polynyas have appeared more than 200-300 times in only a few regions, including NOW, Davis and FJL.

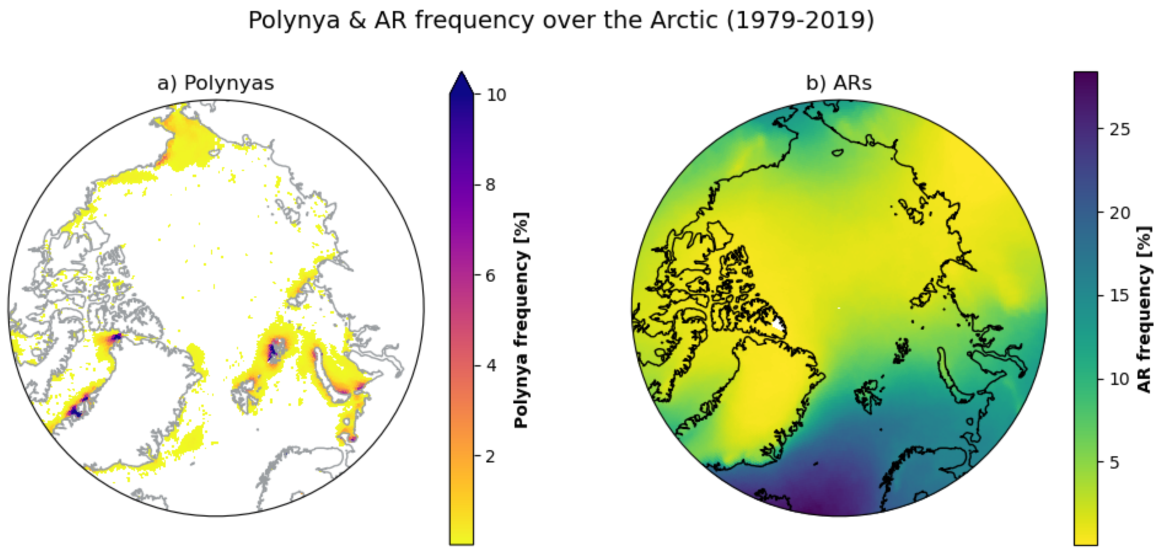

Figure 3: Frequency of polynyas (a) and ARs (b) across the Arctic region between 1979 and 2019.

Figure 3 is showing frequencies and can therefore only represent how common either phenomena is over the Arctic during the whole time period. Further analysis over time will reveal trends, patterns and possible correlations between ARs and polynyas.

5.1.2 Trends in polynya and AR activity over time

In Figure 4, a positive trend can be seen for both ARs and polynyas. The monthly means show an increase in ARs around 11% and polynyas 450%, a significant increase in polynyas. Besides an increase in polynyas, there is a noticeable shift in fluctuations around year 1989. Between 1979 and 1989 there is less fluctuation compared to the rest of the time period. This is especially prominent in the polynya activity, that is relatively stable around 0.5%. After 1989 both phenomena fluctuate more heavily and appear to have several peaks coinciding.

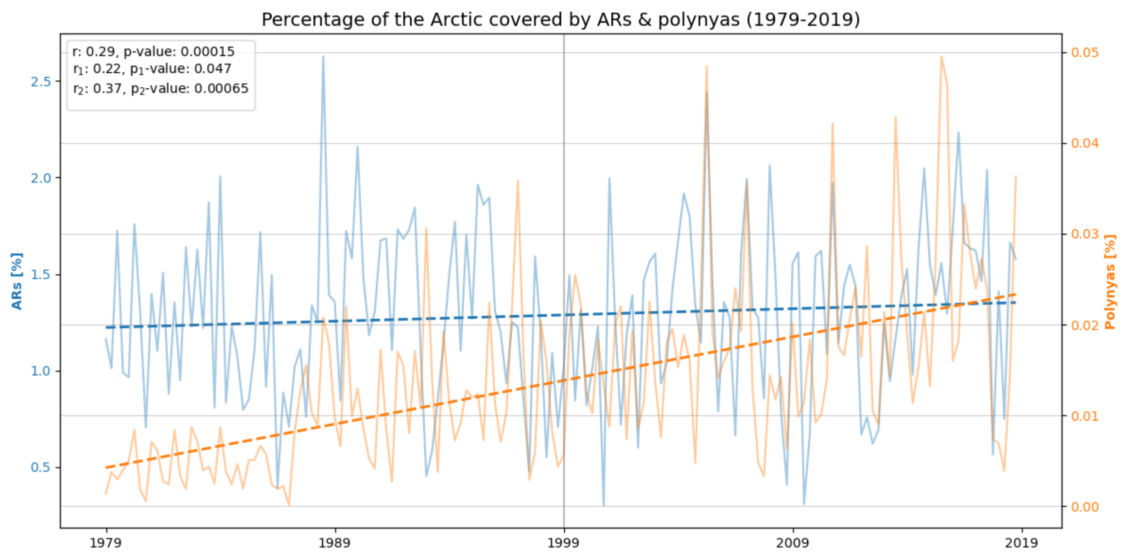

Figure 4: The percentage of the Arctic covered by ARs and polynyas, expressed as monthly means between the years 1979 and 2019, visualized with a blue and orange line respectively. The dashed lines are trendlines for each phenomena. Correlation coefficients and p-values are shown for the entire period as well as divided into the first and second halves of the 40 year period.

To further analyze the fluctuations over the time period in Figure 4, the Pearson correlation coefficient and p-value have been calculated for the first (r_1, p_1) and last (r_2, p_2) 20 years respectively, as well as for the entire period. The overall correlation $r = 0.29$ is significant, and indicates a moderate positive correlation between ARs and polynyas. For the first 20 years, the correlation is lower than observed for the entire period ($r_1 = 0.22$), with a p-value just under the limit for significance ($p_1 = 0.047$). This further indicates a weak relationship between the phenomena. For the last 20 years, the correlation is significantly higher than both the entire period and the first half alone ($r_2 = 0.37$), suggesting a stronger correlation. These results align with observations of Figure 4.

5.2 ARs effect on polynya openings

The following section presents our results and analyses regarding the relationship between AR activity and polynya openings. First, the results from studying the Arctic as a whole is presented and second, a similar regional analysis. Note that throughout this section the only considered polynya activity is the opening event.

5.2.1 Arctic analysis

5.2.1.1 Correlation between ARs and polynya openings

Our results in Figure 4 suggests that ARs and polynyas correlate to some degree, based on the calculated correlations r. To examine further if polynyas open due to the presence of ARs, we analyze the occurrence of ARs and polynya openings for each season.

From Figure 5 a positive relationship between AR- and polynya opening frequencies can be noted, despite the data being collected from the entire Arctic. Because ARs in this analysis are not confined to the same location as the polynya opening, the spatial relation between the phenomena is not considered. The Pearson coefficient being $r = 0.490$ is interpreted as a moderate positive correlation suggesting a relationship. Based on our calculated p-value, the correlation is also significant. However, without considering spatial variabilities no final conclusion can be derived. This result supports our findings in Figure 4. We also cannot dismiss the possibility of other influencing factors that could have effects on both phenomena.

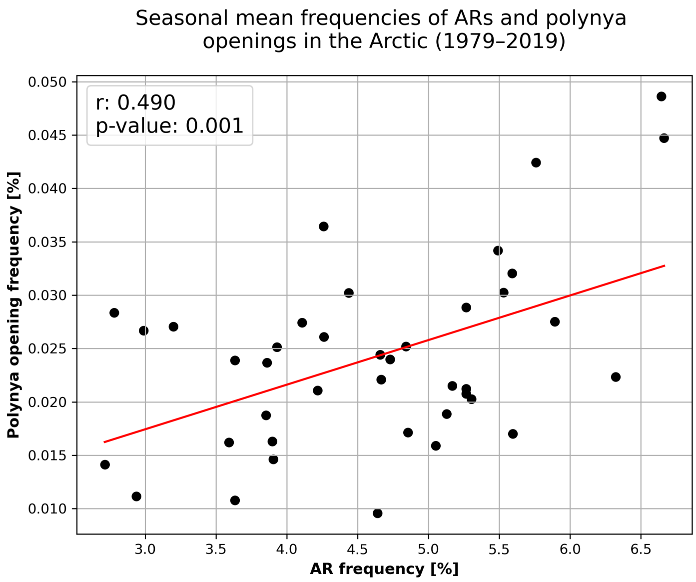

Figure 5: The frequency of ARs and polynya openings from 1979 to 2019, represented with seasonal means for the entire Arctic region. The legend shows the Pearson correlation coefficient and the p-value. A regression line is displayed in red, fitted to the seasonal means.

5.2.1.2 Analysis including temporal aspects and location

Moving on from the more general relationship between ARs and polynya openings, this section presents the results found when studying ARs passing directly above the locations of polynya opening events. Time lag is also investigated in this section, from four days prior to the opening event to the day of opening.

Table 1 shows the percentage of polynya opening events exposed to AR activity compared to the baseline occurrence of ARs on polynya opening locations. The first column shows the percentage of ARs present at polynya opening events, for any of the four upcoming days of the opening. The second column shows the percentage of days over the whole time period that ARs were present at polynya opening locations. We have here defined a polynya opening location as a gridcell that at any point experiences a polynya opening event.

Table 1: Percentage of polynya openings with ARs present prior to opening in comparison to the general prevalence of ARs on polynya opening locations (baseline).

Percentage of polynya openings exposed to AR activity [%]	**Baseline percentage [%]**
36.25	6.74

The results in the first column of Table 1 only considers if an AR has been detected *any* of the upcoming days, not on how many of them. Our results from the first column can be interpreted as "How common it is for ARs to be observed on polynya opening locations *any* of the days prior to an opening event". The content of the second column, referred to as the `baseline percentage`, can be interpreted as "How common ARs are in areas where polynyas have opened up at some point".

When we compare the two columns, it is evident that ARs are much more common in the upcoming days of an opening event compared to how common they are in general for locations where polynyas are known to exist. A difference of almost 30 percentage points can be found and this is an indicator that ARs could be a trigger of polynya openings.

5.2.1.3 Comparison of ARs in polynya opening locations for various time lag days

We can see in Table 2 that ARs are most common on polynya opening locations the day before the opening event. This indicates that the presence of ARs does not always cause the polynya to open instantly but that there can be a delay in time before the effects are seen.

Table 2: Percentage of polynya openings with ARs present for various time lags between 1979 and 2019 [%]. The highest percentage is bolded.

- 4 days	**-3 days**	**-2 days**	**-1 day**	**Opening day**
12.4	13.08	15.42	**18.41**	16.02

When analyzing the results in Table 2, it is important to note that, in contrast to Table 1, there may be overlap between AR and polynya locations. This means that if there is an AR present for multiple days prior to the same polynya opening event, it is here included in all the affected columns. Because of this, the percentages of all four columns can not be added together to calculate the total percentage of polynyas with ARs present the upcoming days, as the same opening event may be included in multiple columns.

We can also see that a majority of polynya openings do not occur during the passing of an AR. The day before the opening event when ARs seems to have the largest impact, 81.6% of polynya opening events do not experience an AR passing. This can be explained by the fact that polynyas are a naturally occurring phenomena in the Arctic. The opening of a polynya can be triggered by various mechanisms and ARs are therefore not a necessary condition.

5.2.2 Regional analysis

This section will look at smaller regions to gain a better understanding of the relationship between ARs and polynya openings. Resembling findings could validate tendencies that have already been observed. The regional analysis will follow the same structure as the Arctic analysis in Section 5.2.1.

From Figure 3 (a) and 6 (a) we see that the amount of polynyas and polynya openings are seemingly proportional in our chosen regions. This implies that polynyas stay open for the same duration in all our regions. Apart from showing proportional frequencies, Figure 3 (a) and 6 (a) show the same distribution of polynyas and polynya openings in the regions, which is to be expected. This is because polynya openings are illustrated in both Figure 6 (a) and 3 (a) , while the days the polynyas stay open is only included in Figure 3 (a).

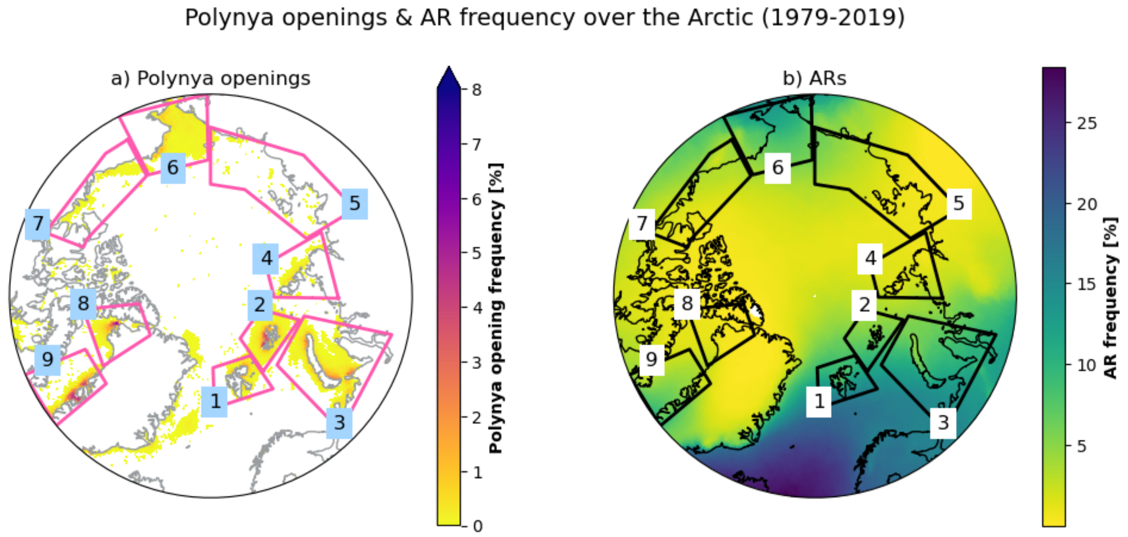

Number	Region
1	Svalbard
2	Franz Josef Land (FJL)
3	Kara Sea
4	Laptev Sea
5	East Siberian Sea (ESS)
6	Chukchi Sea
7	Beaufort Sea
8	North Open Water (NOW)
9	Davis Strait

Figure 6: The identified regions displayed over maps of the frequency of polynya openings (a) and ARs (b) across the Arctic for each grid cell between 1979 and 2019.

5.2.2.1 Correlation between ARs and polynya opening

The results in Figure 7 are an indication as to if the amount of ARs affect the amount of polynya openings. In six of these nine regions the correlation is positive, while the regions ESS, Laptev and Davis (Figure 7 (d),(e),(i)) feature a negative correlation.

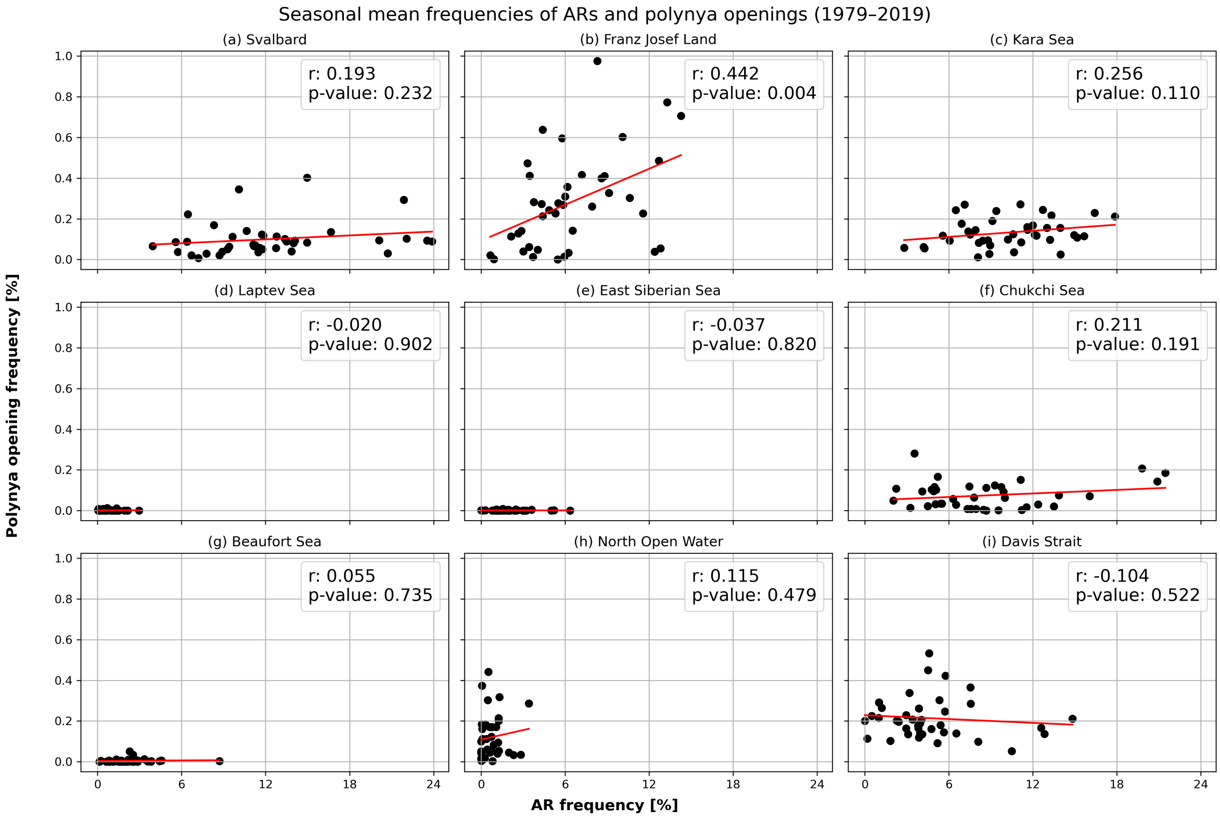

Figure 7: The frequency of ARs and polynya openings from 1979 to 2019, represented with a seasonal mean for all nine regions of interest. In each plot a regression line in red is featured. The Pearson correlation coefficient (r) and p-value are displayed for each region.

The regions Laptev, ESS and Beaufort all have an r-coefficient close to zero (see Figure 7 (d),(e),(g)). As stated in Section 2, a r-coefficient close to zero indicates very low or non-linear correlation. These three regions also differ from the rest by having significantly lower polynya opening frequencies (see Figure 6).

The highest correlations are found in Svalbard, FJL, Kara and Chukchi (see Figure 7 (a),(b),(c),(f)). A high correlation coincides with high concentrations of polynya openings and ARs (see Figure 6) throughout the region. These observations together with the results in Figure 7 suggest a positive correlation between the amount of ARs and polynya openings in areas where both phenomena are prevalent.

Figure 6 ((h),(i)) shows that Davis and NOW also seem to contain numerous polynya openings, but slightly less ARs compared to the regions with higher correlations found in Figure 7. The correlations in Davis and NOW are low (and even negative in Davis), contradicting our previous hypothesis about the relation between ARs and polynya openings. Although, it is still important to note the difference in AR occurence.

There are only a handful of polynya openings in the three regions Laptev, ESS, and Beaufort, and the uncertainties associated with these correlations are considerably large (see Figure 7). The differences in our results could be from regional differences, where some regions could naturally be characterized by lower polynya frequency than others.

It is important to have in mind that in this correlation analysis, in accordance with the Arctic correlation analysis in section 5.2.1.1, the locations of ARs and polynya openings are not taken into account. This means that ARs could be located anywhere in the region, not necessarily in close vicinity of polynya opening locations. Furthermore, each subplot is calculated over the entire chosen region. These regions are chosen because of their high polynya frequency, but will include varying amounts of land where ARs can be present but polynyas cannot, which can affect our results. Figure 8 allows for a better comparison between the regions by displaying them together.

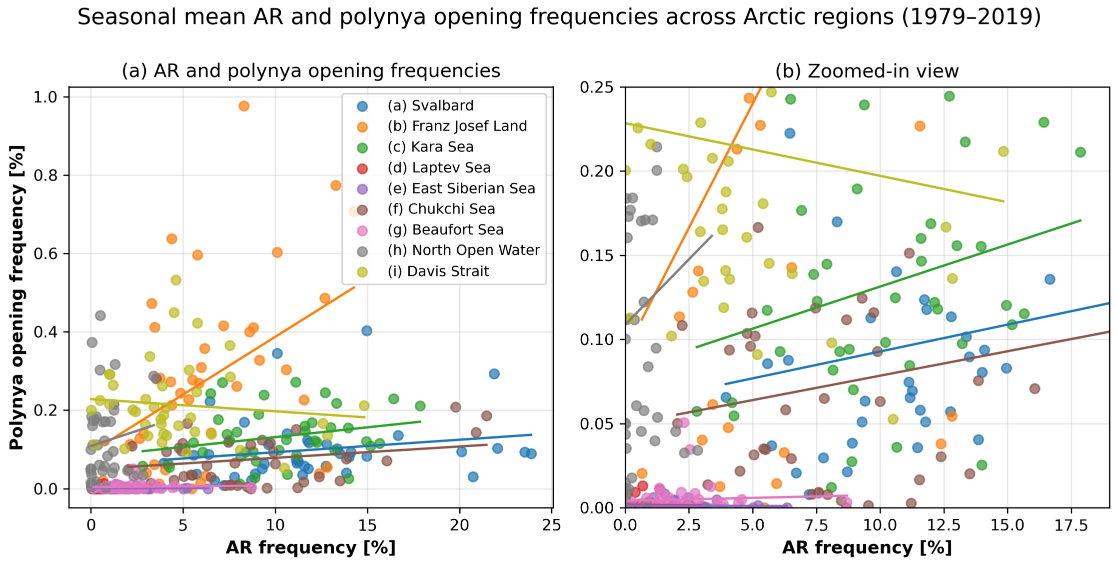

Figure 8: Frequency of ARs and polynya openings from 1979 to 2019, represented with a seasonal mean for all nine regions of interest. All regions are displayed with corresponding regression lines, for easier comparison. Figure 6b) is a magnification of Figure 6a).

The regions Svalbard, FJL, Kara, Chukchi and NOW show positive correlations of varying degrees. In Figure 8 this positive trend of more polynya openings, possibly due to an increasing amount of ARs, seem to reveal itself only when the amount of openings is large enough. This could imply that more opening events may contribute to even more opening events, suggesting a positive feedback loop. Davis is contradicting these five regions by having a high polynya opening frequency but still showing a negative correlation.

The results in Figure 5, 7 and 8 all visualize our results using seasonal mean values. The 40 datapoints are not related in time and are therefore in no way dependent or connected to each other.

5.2.2.2 Analysis including temporal aspects and location

In this section, results from ARs located in the same grid cells as polynya openings the days before the opening event are presented and analyzed for each region.

Table 3 shows the percentage of polynya openings events exposed to AR activity compared to the baseline AR occurrence on polynya opening locations for each of the studied regions. The first column shows the percentage of polynya opening events for which ARs have been present any of the four upcoming days and on the day of the event for each region. The second column is the percentage of time that ARs are present on polynya opening locations, over the whole time period.

Table 3: Percentage of polynya openings with ARs present prior to opening compared to the general prevalence of ARs on polynya opening locations (baseline), for each region.

Region	Percentage of polynya openings exposed to AR activity [%]	Baseline percentage [%]
Svalbard	41.25	10.98
Franz Josef Land	44.04	6.22
Kara Sea	50.23	9.76
Laptev Sea	4.4	1.0
East Siberian Sea	19.29	3.08
Chukchi Sea	32.62	8.45
Beaufort Sea	20.33	2.51
North Open Water	3.41	0.96
Davis Strait	18.54	5.21

Similar to the Arctic analysis in Section 5.2.2.2, the first column can be understood as "How common it is that ARs are observed on the opening locations in the upcoming days of a polynya opening event". The second column can be understood as "How common ARs are in general in areas where polynyas tend to open", or the baseline percentage.

All regions experience an increase in number of ARs over polynya opening locations the days before an opening event occurs compared to how common it is that ARs are detected on these locations in general. However, there are some locations where the increase is greater, for example Kara and FJL.

Something that is worth pointing out is that the regions with the highest increase in percentage points; Kara, FJL and Svalbard, are adjacent to each other. Furthermore, the baseline percentages for these regions (together with Chukchi) are also higher compared to the other regions, aligning with the high AR frequency shown in Figure 6. Furthermore, it is worth mentioning that in Kara more then half of the polynya openings happened with an AR present the days before or on the day of the opening event.

5.2.2.3 Comparison of ARs on polynya opening locations for various time lag days

The occurrence of ARs on polynya opening locations the days before the opening events differ between the regions (see Table 4). The regions ESS and FJL experience an increase of over 10 percentage points between day -4 and -1. This is a larger increase than what the entire Arctic experiences at around 6 percentage points (see Table 2). However, there are regions with very small to no increases in ARs the upcoming days of the opening event. See for example NOW, where there is a slight decrease in ARs the days leading up to the polynya opening event.

Table 4: Percentage of polynya openings with ARs on the polynya opening locations in our chosen regions, 1979-2019 [%], The highest percentage value is bolded for each region

Region	- 4 days	-3 days	-2 days	-1 day	Opening day
Svalbard	16.87	20.29	**20.39**	18.91	15.52
Franz Josef Land	11.73	12.32	16.34	**22.83**	18.98
Kara sea	19.67	18.97	22.21	**24.73**	21.55
Laptev Sea	1.33	0	0	2.13	**2.67**
East Siberain Sea	5.48	3.1	4.52	**17.62**	15.95
Chukchi sea	16.92	18.74	19.84	**22.18**	21.95
Beaufort Sea	4.01	4.38	1.66	8.47	**10.28**
North Open Water	**1.36**	1.32	0.38	0.84	0.82
Davis Strait	5.43	5.44	6.31	5.79	**7.15**

The regions ESS and FJL, which experience the two largest increases in ARs the days before the opening events, differ in several ways. First of all, they are not located close to each other. Second, Figure 6 shows that FJL is a small region with high polynya opening frequency over the entire region. FJL consists of an archipelago with a lot of coastline and a high polynya frequency, whilst ESS is a larger region with lower polynya frequency. The few polynyas that have been present in ESS are small and distributed sparsely across the region. ESS is also a region with a high amount of mainland where ARs can be present but polynyas cannot.

Many of the regions; Kara, Beaufort, Chukchi and Svalbard, experience an increase of approximately 4-6 percentage points of ARs on polynya opening locations during the upcoming days of the polynya opening. This is approximately the same increase as for the Arctic region as a whole (see Table 2).

Two regions that do not exhibit the same pattern as the others; Davis and NOW, are closely located and isolated from other regions (see Figure 6). This raises the question of how this area of the Arctic differs from other regions. Despite not showing a notable increase the upcoming days in Table 4, they still display a high frequency of polynya openings in Figure 6. This indicates that ARs might not have the same effect on polynya openings in this area. For Davis Strait, this theory aligns with the analysis to Figure 7.

Further comparisons can be made between the contents of Table 4 and the baseline values in Table 3. For Davis and NOW the percentages are close to their baseline values for all upcoming days, while the other regions differ more from their baseline. Percentages similar to the baseline all upcoming days suggests that the polynyas there are not affected much by ARs. In ESS, on the other hand, the percentage presented in Table 4 increase drastically one day before an opening event. This suggests that when ARs are present they have a large effect on the openings.

5.3 Summary and discussion

The Arctic analysis reveals a relationship between polynya openings and ARs, both when comparing the frequencies of the phenomena for several seasons (Figure 5) and when looking at the increase of ARs over polynya opening locations the days before opening events (Table 1 and 2). The results imply that the presence of ARs can trigger polynya opening events, and therefore that the poleward shift of ARs might be one of the reasons for the increase of polynyas in the Arctic over the last four decades (Figure 4). A continuous increase of ARs could potentially lead to even more polynyas. As mentioned in Section 2.3.2 several previous studies suggests that the presence of ARs increase the melting of ice in the Arctic. Furthermore, it is important to have in mind that polynyas are more prone to form as the sea ice thickness decrease. In the future, this might cause polynyas to expand and open up in new places, as the ice sheet gets thinner due to increased AR activity.

Moving on to the regional analysis, our results reveal different degrees of correlations between ARs and polynya openings in the studied regions, suggesting that regional differences play an important part. All regions have different ocean current patterns and geographic and topographic attributes, which create unique environments.

As mentioned in section 2.3.1, some regions, like NOW and Davis, experience strong winds and high levels of ice stress. NOW is showing a positive correlation and has a relatively high polynya opening frequency, but second to lowest AR frequency. Davis on the other hand is showing a negative correlation, but still has a high polynya opening frequency and a higher AR frequency than NOW does. Davis is located along the seasonal ice edge of the Arctic, which could increase uncertainties in ice measurements, possibly yielding an overestimated polynya opening frequency. This could explain why our results in Davis contradict the other regions.

One factor that strengthens the hypothesis of an overestimation in polynyas is that the seasonal salinity increase in Davis is one of the lowest out of all regions (see Section 2.3.1). The salinity should increase in regions with polynyas, since polynyas are places of high ice production, which in turn increases the salinity (Section 2.1). If the opening frequency however is not overestimated, the negative correlation in Davis could be due to other drivers affecting polynyas there, more than ARs. From previous research we have found that Baffin Bay, which includes NOW and Davis, experience cold currents and strong winds possibly affecting the polynyas there 2.3.1. Davis is also located along the Greenland coast and could be affected by valley glaciers (Section 2.3.1) or the melting of glaciers possibly diluting the ocean with freshwater.

Svalbard, FJL and Kara are all influenced by the North Atlantic Drift which may be a reason why these regions have slightly more polynya openings in the late winter/early spring (Section 2.3.1). These regions also (together with Chukchi) show the strongest positive correlation between the seasonal frequency of ARs and polynyas (see Figure 7) and the largest increase in AR activity the days before the opening event (see Table 3 and Table 4). This leads us to believe that ARs are also more active later in the winter season in these regions.

Two seemingly similar regions, geographically, are ESS and Beaufort, stretching along long coastlines. From our results in Figure 7, we can see that the correlation between seasonal AR and polynya frequency in ESS is negative, while the correlation in Beaufort is positive, but still very close to zero. One major difference between the regions is the presence of a gyre in Beaufort, along with high sea ice production. Even though these regions have different signs of the correlation, the correlation is so small it might be negligible.

Looking at the percentage of polynya openings with ARs present the upcoming days of the opening event (Table 3), ESS and Beaufort experiences a similar increase compared to the baseline percentages of ARs over these locations. However, when looking at the upcoming days individually (Table 4) the results differ between the regions. ESS experiences a larger increase the upcoming days (when comparing day -4 with -1) compared to Beaufort (12 & 4 percentage points respectively). A possible explanation to this could be that the gyre in Beaufort keeps sea ice in constant motion, leading to polynyas opening up more easily regardless if an AR is present or not. In ESS, ARs might be the main triggering factor opening polynyas. It is however important to remember that the polynya frequency in these areas are very low (see Figure 6) increasing the uncertainties of the results in these regions.

Moving on to Chukchi, which just as Kara, FJL and Svalbard shows a strong relationship between ARs and polynyas (Figure 4, Table 3 and 4). Chukchi is also a region with high polynya and AR frequency (Figure 6). However, in many aspects, Chukchi differs from other regions that shows high correlation. Firstly, while Kara, FJL and Svalbard are neighbors, located around the Barents Sea, Chukchi is located between the United States and Russia (see Figure 6). Furthermore, as opposed to the polynyas in Kara, FJL and Svalbard, the polynyas in Chukchi open up early in the winter season (Section 2.3.1). Possibly suggesting that ARs are more active in the beginning of the season in this part of the Arctic as well. The reason for this is that to achieve such a high correlation in a region where both phenomena show such a high frequency, it is reasonable to believe that they are active during the same period.

This study investigates ARs effect on polynyas by stuyding polynya openings. By only studying opening events, our results capture the initial opening and expansion of polynyas, but does not differentiate these. An alternative approach would be to define a polynya as a group of neighboring grid cells. This would make it possible to distinguish the initial opening of a polynya from the expansion of an already existing polynya. This approach would have made the results more focused on specific polynyas instead of considering each grid cell in the Arctic.

5.4 Sources of error

5.4.1 From input data

The data used in this report defines AR activity using binary values, confirming only the eventual presence of the phenomenon. Variations surrounding temperature, wind speed, moisture content and such are therefore not considered. Further research into how ARs may vary, and how these specific factors might influence their effect on polynyas, is therefore not possible.

The first eight years of the polynya dataset were missing values for every other day. By having to then assume that there was no polynya activity those days, potential data for a more accurate correlation is lost. Including the missing data could have resulted in a lower correlation between ARs and both polynyas and polynya openings. From Figure 4, we observed less fluctuations during this particular period, and this could be a result of the lost data.

Only one reanalysis product (ERA5) was used for the retrieval of the AR data. Furthermore, only one AR catalogue, based on the GuanWaliser v2 algorithm was used. This leads to uncertainties regarding the AR detection. As detection algorithms use different threshold and geometry requirements, ARs are defined differently for each. Comparing several detection algorithms would have yielded a range in our results. If several algorithms gave similar results this would have further strengthened our analysis.

The criteria used to construct the polynya mask may possibly lead to false detections, where other phenomena are interpreted as polynyas. This was brought up in connection to the region Davis' deviating behavior (see Section 5.2.2.1), and how its location close to the seasonal ice edge could effect the amount of detected activity. This could lead to an overestimation of polynyas.

5.4.2 From our analysis

When conducting the regional analysis, all polynya activity was not contained within the chosen regions. Polynya activity that occurred outside these areas could have a substantial influence on the Arctic results, but were neglected in the regional analysis. If a region contains high amounts of land, it could also have an effect on the polynya frequency, as there can not be any polynyas there, and the frequency could be disproportionately low. This only affects the results in Section 5.2.2.1 and 5.2.1.1 since AR and polynya opening correlations are calculated independently of location. However, when moving on to analyzing AR presence on polynya opening locations in Section 5.2.1.2 and 5.2.2.2, this is no longer a problem.

Some investigated regions were comparatively large with low polynya activity. This could impact the observed frequency of the phenomenon, as measured regional activity will be compared to its size. For example, by dividing a bigger region like ESS, the polynya frequencies in the separated areas would increase. This could give, relative to the other regions sizes, more comparable results even without creating frequencies.

When investigating time lag, the code does not compute any analysis on the initial three days of the polynya dataset. The missing days of possible polynya activity is therefore not studied for time lag correlations. However, this reduction can be seen as negligible, as there in total are 4850 days used in this study.

Pearson's correlation coefficient is best suited for certain instances since; as mentioned in Section 4.5.1, it is very sensitive to outliers. Because of this, the measured correlation coefficient might not give the most accurate representation of the relationship between ARs and polynya openings. It is also rare for a strictly linear relationship to be found in the natural world, and what might be considered a moderate correlation on paper could in actuality mean a strong correlation in our field of study.

6 Conclusion

The aim of our study was to investigate a potential relationship between ARs and Arctic polynyas. This was done by comparing datasets for Arctic polynyas and AR activity between 1979 and 2019, then analyzing the extent of both phenomena in the Arctic as well as their trends over time. Our results shows that Arctic polynyas are most frequent along coasts around Barents Sea, Chukchi Sea and Baffin Bay. This aligns with previous research stating that latent heat polynyas, mainly located along coasts, are the most common type in the Arctic. The results also revealed that ARs are more frequent between latitudes 65-80°, but occur in the entire Arctic region at least a few times during the time period of study. Furthermore, the analysis showed that both AR and polynya activity have increased in the Arctic over the last four decades, which also aligns with previous research.

Our analysis of the entire Arctic region revealed a positive moderate correlation between the seasonal frequency of ARs and polynya openings, independent of location, with the correlation coefficent $r = 0.49$. Furthermore, when studying ARs passing directly over polynya opening locations the days before the opening event we saw an increase of ARs by almost 30 percentage points compared to the baseline occurrence of ARs over these regions. This baseline can be interpreted as "How common ARs are in areas where polynyas have opened up at some point". This increase suggests that ARs do affect polynyas by triggering opening events.

Moving on to the regional analysis, five out of our nine chosen regions follow the same pattern as was found in the Arctic analysis. However, the seasonal frequency correlation of ARs and polynyas independent of location is not as strong for any of the regions as for the whole Arctic. Franz Josef Land shows the strongest correlation $r = 0.442$, followed by Kara Sea with a correlation of $r = 0.256$. There are also regions displaying a negative or low correlation between ARs and polynya openings. These are Laptev Sea, East Siberian Sea, Beaufort Sea and Davis Strait. For all nine regions, AR activity on the opening locations increases the days before the opening event compared to their respective baselines. This increase also varies between the regions, where Kara Sea and Franz Josef Land experiences the largest increase.

There are large variations in AR and polynya frequencies between the regions. From our results, we can see that regions with high polynya and AR frequency generally display higher correlations in comparison to those with low frequencies. However, there are regions that this does not apply to, for example Davis Strait and East Siberian Sea. Differences in our results can be due to how other mechanisms that affects polynyas behave in these regions, like wind and ocean currents.

Considering sources of error and possible improvements, further and more thorough research is needed. By using binary data, all ARs are assumed to be equally strong. This means that we do not account for the strength of ARs, as these may differ between regions and seasons, potentially affecting polynyas to varying degrees. Furthermore, in this study polynya openings and expansion are not distinguished. Studying these two separately would enable results showing if there is a difference between how ARs affect the initial opening of a grid cell in a limited region compared to expansion of an already open polynya. Studying Arctic phenomena, such as polynyas and ARs, is of great relevance for understanding the Arctic mechanisms and the effects that climate change might have.

7 Bibliography

Armstrong, T. (1972). World meteorological organization. wmo sea-ice nomenclature. terminology, codes and illustrated glossary. edition 1970. geneva, secretariat of the world meteorological organization, 1970.[ix], 147 p.[including 175 photos]+ corrigenda slip.(wmo/omm/bmo, no. 259, tp. 145.) *Journal of Glaciology*, *11*(61), 148–149.

Berman, J. J. (2016). Chapter 4 - understanding your data. In *Data simplification* (pp. 135–187). Morgan Kaufmann. https://doi.org/https://doi.org/10.1016/B978-0-12-803781-2.00004-7

Copernicus Climate change service. (n.d.). *Climate reanalysis* [[Online.]]. https://climate.copernicus.eu/climate-reanalysis

European Centre for Medium-Range Weather Forecasts. (2025). *Fact sheet: Earth system data assimilation*. https://www.ecmwf.int/en/about/media-centre/focus/2025/fact-sheet-earth-system-data-assimilation

Faizi, N., & Alvi, Y. (2023). Chapter 6 - correlationfor datasets, please refer to companion site: Https://www.elsevier.com/books-and-journals/book-companion/9780443185502. In *Biostatistics manual for health research* (pp. 109–126). Academic Press. https://doi.org/https://doi.org/10.1016/B978-0-443-18550-2.00002-5

Francis, D., Mattingly, K. S., Temimi, M., Massom, R., & Heil, P. (2020). On the crucial role of atmospheric rivers in the two major weddell polynya events in 1973 and 2017 in antarctica. *Science advances*, *6*(46), eabc2695.

Guan, B., & Waliser, D. (2015). Detection of atmospheric rivers: Evaluation and application of an algorithm for global studies. *Journal of Geophysical Research: Atmospheres*, *120*(24), 12514–12535.

Guan, B., & Waliser, D. (2019). Tracking atmospheric rivers globally: Spatial distributions and temporal evolution of life cycle characteristics. *Journal of Geophysical Research: Atmospheres*, *124*(23), 12523–12552.

Haacker, J., Wouters, B., Fettweis, X., Glissenaar, I., & Box, J. (2024). Atmospheric-river-induced foehn events drain glaciers on novaya zemlya. *Nature Communications*, *15*(1), 7021.

Hersbach, H., Bell, B., Berrisford, P., Hirahara, S., Horányi, A., Muñoz-Sabater, J., Nicolas, J., Peubey, C., Radu, R., Schepers, D., et al. (2020). The era5 global reanalysis. *Quarterly journal of the royal meteorological society*, *146*(730), 1999–2049.

Kim, Y., Kim, T.-H., & Ergün, T. (2015). The instability of the pearson correlation coefficient in the presence of coincidental outliers. *Finance Research Letters*, *13*, 243–257. https://doi.org/https://doi.org/10.1016/j.frl.2014.12.005

Kump, L., Kasting, J., & Crane, R. (2014). *Latex: The earth system* (3rd). Pearson New International Edition.

Li, L., Cannon, F., Mazloff, M., Subramanian, A., Wilson, A., & Ralph, F. M. (2024). Impact of atmospheric rivers on arctic sea ice variations. *The Cryosphere*, *18*(1), 121–137.

Li, Z., & Ding, Q. (2024). A global poleward shift of atmospheric rivers. *Science Advances*, *10*(41), eadq0604.

Ma, W., Wang, H., Chen, G., Qian, Y., Baxter, I., Huo, Y., & Seefeldt, M. W. (2024). Wintertime extreme warming events in the high arctic: Characteristics, drivers, trends, and the role of atmospheric rivers. *Atmospheric Chemistry and Physics*, *24*(7), 4451–4472.

Mattingly, K., Mote, T., & Fettweis, X. (2018). Atmospheric river impacts on greenland ice sheet surface mass balance. *Journal of Geophysical Research: Atmospheres*, *123*(16), 8538–8560.

McGuire, A. D., Anderson, L. G., Christensen, T. R., Dallimore, S., Guo, L., Hayes, D. J., Heimann, M., Lorenson, T. D., Macdonald, R. W., & Roulet, N. (2009). Sensitivity of the carbon cycle in the arctic to climate change. *Ecological monographs*, *79*(4), 523–555.

Morales Maqueda, M. A., Willmott, A. J., & Biggs, N. (2004). Polynya dynamics: A review of observations and modeling. *Reviews of Geophysics*, *42*(1).

Previdi, M., Smith, K. L., & Polvani, L. M. (2021). Arctic amplification of climate change: A review of underlying mechanisms. *Environmental Research Letters*, *16*(9), 093003.

Priest, R. (2005). Statistical/substantive, interpretations and data limitations. In K. Kempf-Leonard (Ed.), *Encyclopedia of social measurement* (pp. 671–674). Elsevier. https://doi.org/https://doi.org/10.1016/B0-12-369398-5/00180-8

Rantanen, M., Karpechko, A. Y., Lipponen, A., Nordling, K., Hyvärinen, O., Ruosteenoja, K., Vihma, T., & Laaksonen, A. (2022). The arctic has warmed nearly four times faster than the globe since 1979. *Communications earth & environment*, *3*(1), 168.

Reid, N. (2001). Significance, tests of. In N. J. Smelser & P. B. Baltes (Eds.), *International encyclopedia of the social behavioral sciences* (pp. 14085–14091). Pergamon. https://doi.org/https://doi.org/10.1016/B0-08-043076-7/00506-4

Schauer, U., & Fahrbach, E. (1999). A dense bottom water plume in the western barents sea: Downstream modification and interannual variability. *Deep Sea Research Part I: Oceanographic Research Papers*, *46*(12), 2095–2108.

Schuur, E. A., Bockheim, J., Canadell, J. G., Euskirchen, E., Field, C. B., Goryachkin, S. V., Hagemann, S., Kuhry, P., Lafleur, P. M., Lee, H., et al. (2008). Vulnerability of permafrost carbon to climate change: Implications for the global carbon cycle. *BioScience*, *58*(8), 701–714.

Service, C. C. C. (2023). Complete era5 global atmospheric reanalysis. https://doi.org/10.24381/cds.143582cf

Shepherd, A., Ivins, E. R., A, G., Barletta, V. R., Bentley, M. J., Bettadpur, S., Briggs, K. H., Bromwich, D. H., Forsberg, R., Galin, N., et al. (2012). A reconciled estimate of ice-sheet mass balance. *Science*, *338*(6111), 1183–1189.

Shields, C. A., Marquardt Collow, A. B., Guan, B., Kim, S., Manuel Lora, J., McClenny, E. E., Nardi, K. M., Payne, A. E., Reid, K. J., Jay Shearer, E., Tome, R., Wille, J. D., Ramos, A. M., Gorodetskaya, I. V., Leung, R., Allen O'Brien, T., Martin Ralph, F., Rutz, J. J., Ullrich, P. A., & Wehner, M. F. (2022). Atmospheric River Tracking Method Intercomparison Project Tier 2 Reanalysis Source Data and Catalogues. https://doi.org/10.26024/rawv-yx53

Shields, C. A., Rutz, J. J., Leung, L.-Y., Ralph, F. M., Wehner, M., Kawzenuk, B., Lora, J. M., McClenny, E., Osborne, T., Payne, A. E., et al. (2018). Atmospheric river tracking method intercomparison project (artmip): Project goals and experimental design. *Geoscientific Model Development*, *11*(6), 2455–2474.

Smith, S., Muench, R., & Pease, C. (1990). Polynyas and leads: An overview of physical processes and environment. *Journal of Geophysical Research: Oceans*, *95*(C6), 9461–9479.

Tamura, T., & Ohshima, K. I. (2011). Mapping of sea ice production in the arctic coastal polynyas. *Journal of Geophysical Research: Oceans*, *116*(C7).

Temizel, A., Halici, T., Logoglu, B., Temizel, T. T., Omruuzun, F., & Karaman, E. (2011). Chapter 34 - experiences on image and video processing with cuda and opencl. In W.-m. W. Hwu (Ed.), *Gpu computing gems emerald edition* (pp. 547–567). Morgan Kaufmann. https://doi.org/https://doi.org/10.1016/B978-0-12-384988-5.00034-6

Winsor, P., & Björk, G. (2000). Polynya activity in the arctic ocean from 1958 to 1997. *Journal of Geophysical Research: Oceans*, *105*(C4), 8789–8803.

Wong, C. H. M., & Heuzé, C. (2025). Daily Arctic polynya masks 1978-2024 from two satellite sea ice products (SMMR, SSM/I & SSMIS and SMOS & SMOS-SMAP). https://doi.org/10.1594/PANGAEA.987383

Wong, C. H. M., Heuzé, C., Ickes, L., & Zhou, L. (2026). The spatio-temporal variability, trends, and drivers of winter arctic polynyas. *Journal of Climate*, e250312.

Zhang, P., Chen, G., Ting, M., Ruby Leung, L., Guan, B., & Li, L. (2023). More frequent atmospheric rivers slow the seasonal recovery of arctic sea ice. *Nature Climate Change*, *13*(3), 266–273.

Zhang, Y., Zhang, Y.-Y., Xu, D.-Y., Chen, C.-S., Shen, X.-Y., Hu, S., Chang, L., Zhou, X.-Q., & Feng, G.-P. (2021). Impacts of atmospheric and oceanic factors on monthly and interannual variations of polynya in the east siberian sea and chukchi sea. *Advances in Climate Change Research*, *12*(4), 527–538.

Zhang, Z., Ralph, F. M., & Zheng, M. (2019). The relationship between extratropical cyclone strength and atmospheric river intensity and position. *Geophysical Research Letters*, *46*(3), 1814–1823.

Zhu, Y., & Newell, R. E. (1998). A proposed algorithm for moisture fluxes from atmospheric rivers. *Monthly weather review*, *126*(3), 725–735.